Simulation of Mechanical Test in Digital Rock Affected by Rock Heterogeneity and Flow in Porous Media

Wenjie Ma, Yongfei Yang*

School of Petroleum Engineering, China University of Petroleum (East China)

Abstract: As the main reservoir of oil and gas resources, the physical and mechanical properties of the rock are complicated. The strong heterogeneity of rock and the flow in porous media further influences the nature of stress propagation. Therefore, considering the heterogeneous particle model and fluid-structure coupling, it is very important to study the variation law of rock mechanical properties under a stress state, which lays a foundation for formation fracturing and mining. In this paper, the mechanical properties of the rock are studied by the ideal, heterogeneous, and flow models in porous media. The results show that the stress of the contact surface between particles of the same size is large. Still, the stress of the contact surface between different particles is larger, which is more likely to become the weak mechanical link of failure. When the displacement of the z-axis is the same, the x and y-axis increase the axial stress of the z-axis. The peak stress is high and more sensitive when the particle size difference is small. When water is in the pores, the rock strength obtained under consolidated undrained is greater than that under consolidated drained.

1. Introduction

As the main reservoir of oil and gas resources, the rock particle structure is complex, the mineral composition is diverse, and the physical and mechanical properties of the rock are diverse. Rock mineral particles' shape, surface, and bonding mode are different, and rock heterogeneity is strong. The existence of defects such as pores, cracks, and bedding in the rock enhances the heterogeneity of the rock and further influences the nature of stress propagation. The flow in the porous media of rocks can affect the physical properties of rocks.

The uneven composition and structure of natural rocks greatly affect their mechanical properties of rocks. Heterogeneity has different influences on the mechanical properties of different types of rocks, such as shale [2], metamorphic rock [4], and sandstone, and also affects the stability of civil engineering, underground mining structure [3] and hydraulic fracturing [9].

The flow in the porous media of rocks can affect the physical properties of rocks. In the conventional triaxial test, pore water pressure changes of rock under different environments are measured by consolidated drained [6], consolidated undrained [7] and unconsolidated undrained [8].

The strong heterogeneity of rock and the flow in porous media further influences the nature of stress propagation. Therefore, considering the heterogeneous particle model and fluid-structure coupling to study the variation law of rock mechanical properties under a stress state, lay a foundation for fracturing and mining in the formation. In this paper, the mechanical properties of the rock are studied by the ideal, heterogeneous, and flow models in porous media.

2. Methodology

Firstly, the equilibrium equation is as follows:

$$\rho \frac{\partial^2 \mathbf{u}}{\partial t^2} = \nabla \cdot \sigma + \mathrm{F_v} \tag{1}$$

where F_v is area force, σ is stress and $\boldsymbol{u}$ is velocity field.

According to the principle of minimum energy, the elastic free energy matrix is solved to solve the displacement of each pixel. The elastic potential energy of each voxel can be expressed as:

$$E_n = \frac{1}{2}\int d^3 r \varepsilon_{pq} C_{pqkl} \varepsilon_{kl} \tag{2}$$

where E_v is the elastic potential energy of the system, ε_{pq} and ε_{kl} are the strain tensor, and C_{pqkl} is the elasticity tensor. Considering the fluid-structure coupling, laminar flow is added. Incompressible fluids are used because the pore volume is small and the fluid deformation is small. From the basic momentum equation [5], we can derive the following:

$$\rho\left(\mathbf{u}_{\text{fluid}} \cdot \nabla\right)\mathbf{u}_{\text{fluid}} = \nabla \cdot [-p\mathbf{I} + \mathbf{K}] + \mathbf{F} \tag{3}$$

where ρ is the fluid density, $\mathbf{u}_{\text{fluid}}$ is the fluid velocity field, p is pressure, $\mathbf{K}$ is the stress tensor and $\mathbf{F}$ is volume force.

*Email: yangyongfei@upc.edu.cn

https://doi.org/10.1051/e3sconf/202337001005

The boundary conditions of mirrored symmetric graphs are a combination of Dirichlet boundary conditions and Neumann boundary conditions:

$$\mathbf{K}=\mu\left(\nabla\mathbf{u}_{\text{fluid}}+\left(\nabla\mathbf{u}_{\text{fluid}}\right)^{T}\right) \tag{4}$$

The rock strength criterion is the Drucker-Prager criterion [1]:

$$F_{\text{cone}}=\sqrt{J_2}+\alpha I_1-k \tag{5}$$

The relationship between elastic modulus can be expressed as:

$$\nu=\frac{3K-2\mu}{2\left(3K+\mu\right)},\quad E=\frac{9K\mu}{3K+\mu} \tag{6}$$

where v is Poisson's ratio, K is volume modulus, μ is elastic modulus and E is Young's modulus.

3. Results and Discussion

3.1. Ideal model

We can calculate a large number of parameters of the model, such as shear modulus, elasticity modulus, and stress-strain curve. We need parameters such as the Diameter of the sample is 10 mm, Young's modulus is 30 GPa, Poisson's ratio is 0.3, the Angle of internal friction is 35 deg, and Cohesion is 20 MPa.

The ideal model three-dimensional digital core is shown in Fig. 1(a). Displacements are applied in all directions of the three dimensions, and the deformation in each direction is calculated. Finally, the stress diagram of the whole geometric structure is obtained, as shown in Fig. 1(b). The model has a simple structure and strong homogeneity, which makes the stress division uniform and agrees well with the actual situation.

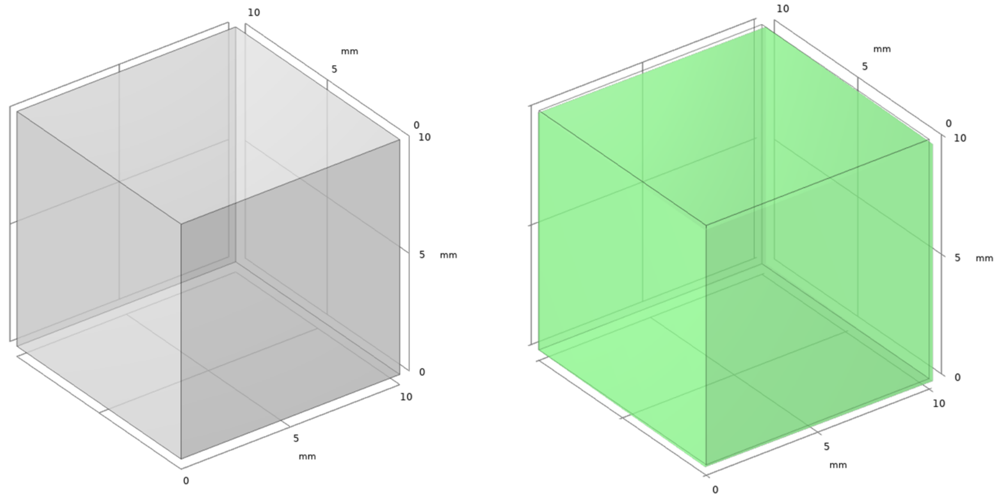

(a) (b)

Fig. 1 3D ideal model image and strain diagram

The calculated stress-strain diagram is shown in Fig. 2. The slope of the elastic region in the stress-strain diagram is the elastic modulus of the sample according to Hooke's law. The slope of the elastic region in the figure is 30 GPa, which is in good agreement with the previously input data. The variation trend is in good agreement with the actual results, which verifies the accuracy and feasibility of the model.

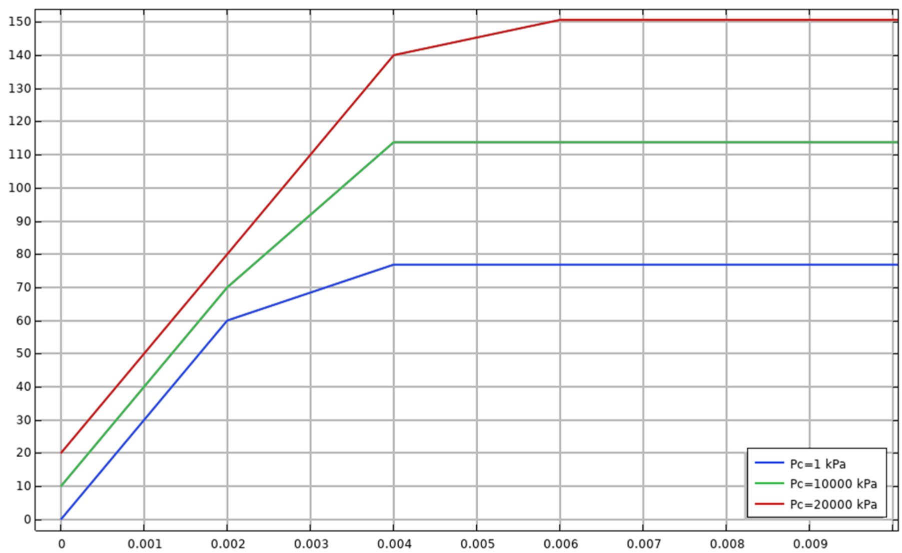

Fig. 2 Stress-strain diagram of ideal model, Pc is the calculated confining pressure

3.2. Rock heterogeneity

The heterogeneity is one of the factors affecting the mechanical properties of rock. The composition and structure of natural rocks are not evenly distributed in all directions, resulting in a large gap in mechanical properties. The particle-based numerical model considers the influence of rock heterogeneity on mechanical properties at the microscopic level, forming a set of digital cores with the upper set particle size different from the lower set, as shown in Fig. 3. Due to the particle size, the difference is too large to meet the actual situation. The specific particle distribution is shown in Table 1. Considering only the heterogeneity of the upper and lower layers, the strain curves of the digital cores in the triaxial stress state are obtained by numerical simulation.

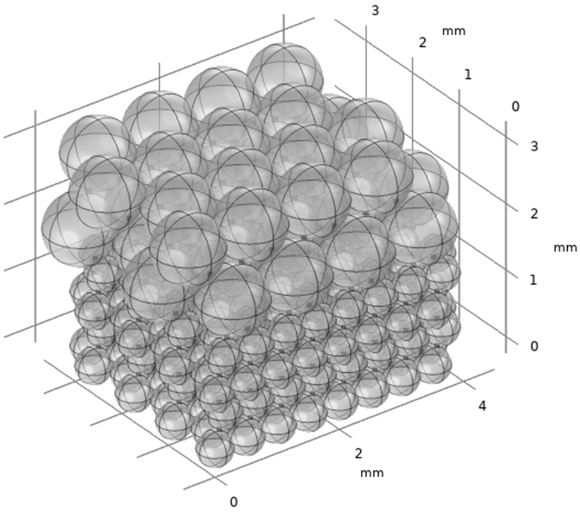

Fig. 3 Model built using the compaction methods with different particle sizes

Table 1 Combinations of different particle sizes

Case No.	Case 1	Case 2	Case 3	Case 4	Case 5
Combinations (mm)	2+1	1+0.5	0.5+0.25	0.25+0.125	0.125+0.0625
Particle size difference (mm)	1	0.5	0.25	0.125	0.0625

To explore the influence mechanism of heterogeneity caused by different particle sizes on rock mechanical properties under a three-dimensional stress state, displacement was applied to the most marginal sphere in the x, y, and z directions. The internal stress strain was calculated, and the stress diagram was made, as shown in Fig. 4. It can be seen from the figure that the stress of the contact surface between particles of the same size is large. Still, the stress of the contact surface between different particles is larger, which is more likely to become the weak mechanical link of failure.

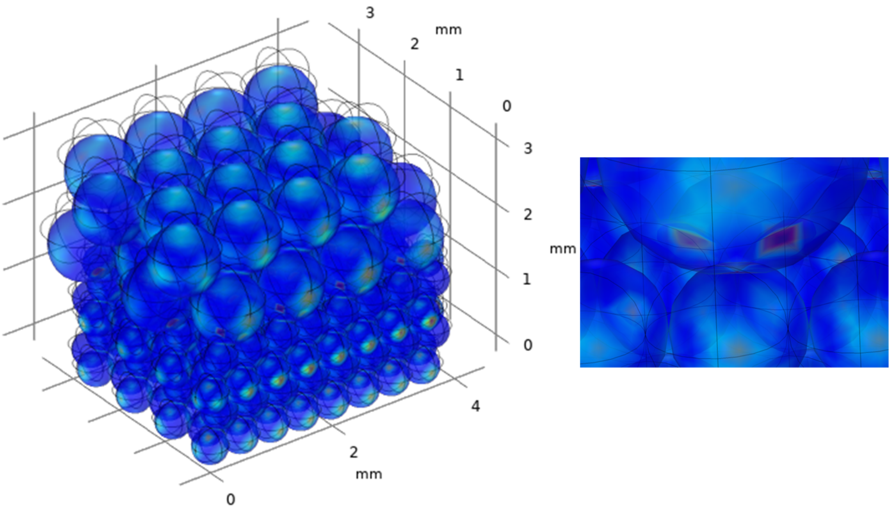

Fig. 4 Simulation strain diagram of case3, the detailed diagram on the right

The simulation results were analyzed, and the stress-strain curve was drawn, as shown in Fig. 5. By comparing the curves ① and ②, when the displacement of the z-axis is the same, the displacement of the x and y-axis increases the axial stress of the z-axis. By comparing the curves ② and ③, the displacement of the x and y axes consolidated the model, and the peak stress of the z-axis increased. The appearance of the curves ④ and ⑤ is due to the interval of parameter setting. For example, the plastic strain has occurred in this stress state, and the calculation of peak stress failed, so only the results of the previous step are displayed. This error is small and within the acceptable range.

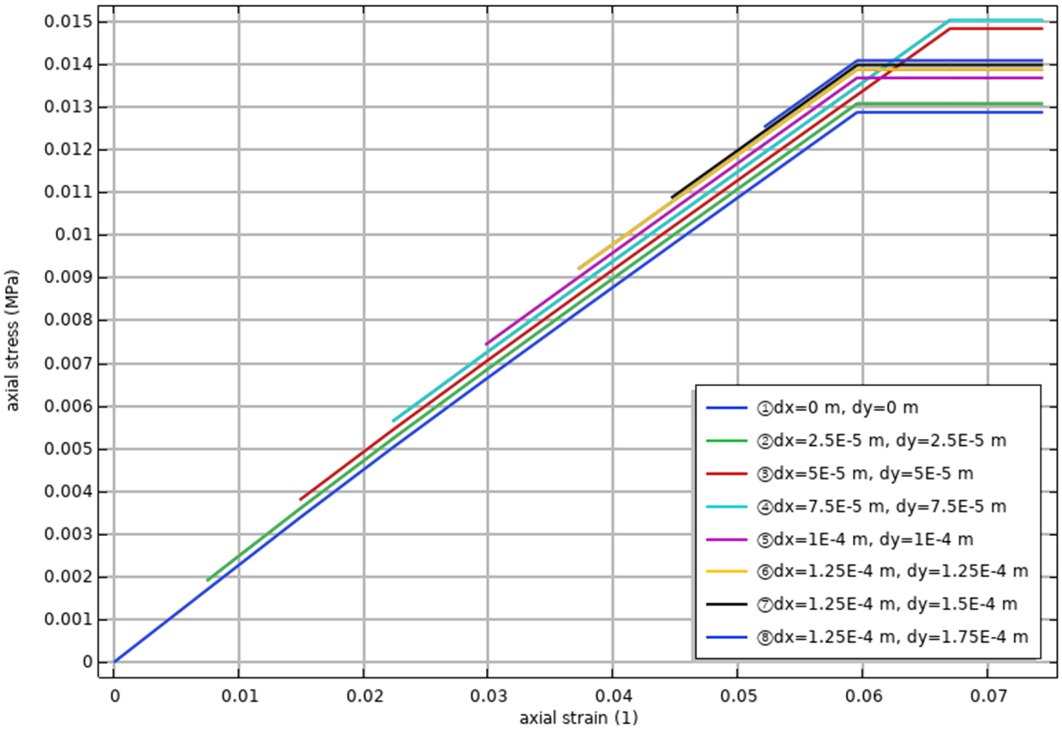

Fig. 5 Stress-strain curve of case 3

By comparing the peak stress obtained by different particle size differences, the curve drawn is shown in Fig. 6. It can be seen from the figure that the relationship between peak stress and the particle size difference is linear. This corresponds well with the actual situation. However, the peak stress is higher and more sensitive when the particle size difference is small. When the particle size difference is large, although the peak stress is relatively high, it is less sensitive.

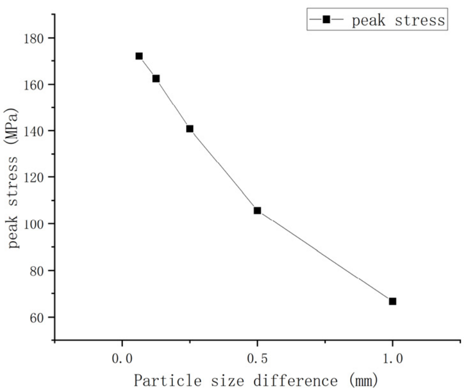

Fig. 6 Peak stress vs. particle size difference

3.3. Flow in porous media

The micro-influencing factors of rock mechanical properties are complex. In addition to the influence of rock heterogeneity brought, flow in porous media also significantly affects the physical properties of rock. The true triaxial test can strictly control drainage conditions and measure the pore water pressure change in the sample. In this section, based on the principle of true triaxial test and considering the fluid-structure coupling, numerical simulation is conducted based on the digital core. And two sets of simulations of consolidated drained and consolidated undrained are designed to compare and study the influence of flow in the porous media on the sample's mechanical properties.

In the same geometric structure, the same parameters were adopted, a laminar flow of pore water was made, and drainage conditions were only controlled. The simulation results are shown in Fig. 7 and Fig. 8. The stress distribution is roughly the same, but some areas still have great differences. This is because pore water pressure has less effect on the stress of the whole geometry, but the wall in contact with the water bears more pressure. When water is in the pores, the rock strength obtained under consolidated undrained is greater than that under consolidated drained.

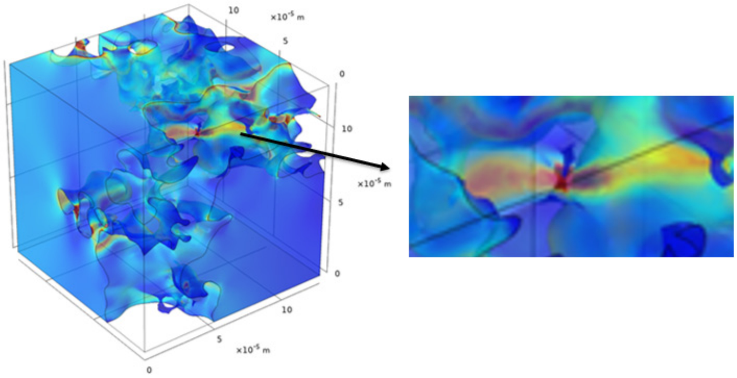

Fig. 7 Simulation strain diagram of consolidated drained, the detailed diagram on the right.

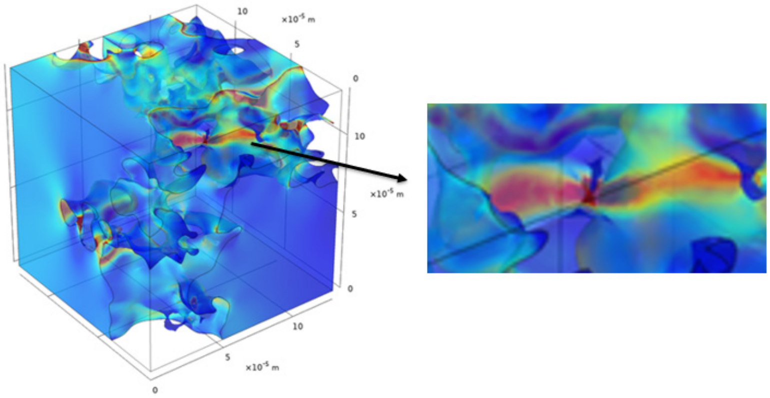

Fig. 8 Simulation strain diagram of consolidated undrained, the detailed diagram on the right

The stress surface is wider in actual crude oil production and should be changed dramatically. However, due to edge water and water injection development in most oil fields, the water area is wide, and the pore water pressure is small for the deformed part of the rock.

4. Conclusions

(1) The variation trend agrees with the actual results.

(2) The stress of the contact surface between particles of the same size is large, but the stress of the contact surface between different particles is larger, which is more likely to become the weak mechanical link of failure.

(3) When the displacement of the z-axis is the same, the displacement of the x and y-axis increases the axial stress of the z-axis.

(4) When the particle size difference is small, the peak stress is high and more sensitive.

(5) When water is in the pores, the rock strength obtained under consolidated undrained is greater than that under consolidated drained.

Acknowledgments

We acknowledge the following financial support: National Natural Science Foundation of China (52034010).

References

[1] Anandarajah, A. (2010). The Drucker–Prager Model and Its Integration. In *Computational Methods in Elasticity and Plasticity* (pp. 513-560). New York, NY: Springer, New York, NY.

[2] Fjær, E., & Nes, O.-M. (2014). The Impact of Heterogeneity on the Anisotropic Strength of an Outcrop Shale. *Rock Mechanics and Rock Engineering, 47*(5), 1603-1611. doi:https://doi.org/10.1007/s00603-014-0598-5

[3] Heng, S., Guo, Y., Yang, C., Daemen, J. J. K., & Li, Z. (2015). Experimental and theoretical study of the anisotropic properties of shale. *International Journal of Rock Mechanics and Mining Sciences, 74*, 58-68. doi:https://doi.org/10.1016/j.ijrmms.2015.01.003

[4] Özbek, A., Gül, M., Karacan, E., & Alca, Ö. (2018). Anisotropy effect on strengths of metamorphic rocks. *Journal of Rock Mechanics and Geotechnical Engineering, 10*(1), 164-175. doi:https://doi.org/10.1016/j.jrmge.2017.09.006

[5] Poirier, D. R., & Geiger, G. H. (2016). Laminar Flow and the Momentum Equation. In D. R. Poirier & G. H. Geiger (Eds.), *Transport Phenomena in Materials Processing* (pp. 39-74). Cham: Springer International Publishing.

[6] Rahman, A. S. A., Noor, M. J. M., Ahmad, J., Zain, N. H. M., & Rosli, M. I. F. (2019). Shear strength behaviour of different energy in compaction using

consolidated drained triaxial test. *IOP Conference Series: Materials Science and Engineering, 513*(1).

[7] Rahmi, A., Taib, S., Sahdi, F., Mapplati, M., & Ghani, M. (2020). Shear Strength Parameters of Cement Stabilized Amorphous Peat of Various Water Additive Ratios at Different Natural Moisture Contents under Consolidated Undrained Triaxial Test. *International Journal of Recent Technology and Engineering (IJRTE), 8*(6).

[8] Yang, K.-H., Yalew, W. M., & Nguyen, M. D. (2016). Behavior of Geotextile-Reinforced Clay with a Coarse Material Sandwich Technique under Unconsolidated-Undrained Triaxial Compression. *International Journal of Geomechanics, 16*(3), 04015083. DOI: https://doi.org/10.1061/(ASCE)GM.1943-5622.0000611

[9] Yang, T. H., Tham, L. G., Tang, C. A., Liang, Z. Z., & Tsui, Y. (2004). Influence of Heterogeneity of Mechanical Properties on Hydraulic Fracturing in Permeable Rocks. *Rock Mechanics and Rock Engineering, 37*(4), 251-275. doi:https://doi.org/10.1007/s00603-003-0022-z